Article

Preferential recruitment of monocyte into the brain is orchestrated by VCAM-1 expression

Wei-Wei Zhu1*, Junyao Wang1*, Qiming Dong2, Lin zhao3#, Jian Chen1#

1 Department of Cardiovascular Medicine, Fifth Affiliated Hospital of Sun Yat-sen University, Zhuhai, Guangdong 519000, China
2 Department of Internal Medicine, Greater Baltimore Medical Center, Towson, Maryland 21204, USA
3 Department of Cardiology, Beijing Anzhen Hospital, Capital Medical University, 100029, Beijing, China
* These authors contribute equally to this study.
# Correspondence: Jian Chen, Email: chenjn@mail.sysu.edu.cn; Lin Zhao, Email: trichina2007@126.com.

Abstract: The restriction of normal blood flow is the cause of many diseases including stroke and coronary artery diseases. To study the consequences of vessel blockade, previous models mainly focused on major arteries and have been well studied. However, the sequela from interruption of capillary vessels by microemboli was less well characterized. In this study, we exploited polystyrene microspheres as a mimicry of microemboli and found that microspheres of this size can be trapped in capillary vessels of all organs without causing apparent acute morbidities of the host. Interestingly, we accidentally found significantly increased recruitment of monocyte to the brain vasculature expressing low levels of Ly6C expression, but not to other organs. Further study revealed the spleen is the major origin of the recruited monocyte. Most importantly, VCAM-1 which is constitutively expressed on mouse brain vasculature orchestrates the recruitment of monocyte. Blockade of VCAM-1 in mice can substantially reduce monocyte recruitment. Interestingly, monocytes get activated through TNF-⍟ signaling which likely happens in the spleen instead of the brain. Collectively, we found a unique monocyte recruitment strategy in the brain comparing to other orangs, in response to capillary blockade induced by polystyrene microspheres.

Keywords: monocyte, VCAM-1, microsphere, capillary vessel, microemboli

Introduction

Blood flow within the capillary vessels is essential for the ambient delivery of oxygen and nutrient supply to terminal organs. However, emboli from various sources can stop the normal flowing blood when it encounters narrowing in blood vessel. This will prevent blood flow to downstream tissues and causes ischemia. Interruption of blood vessels causes a variety of diseases depending on the location of the blockade, such diseases include stroke[1], coronary artery disease[2], pulmonary embolism[3], etc.. These diseases collectively result in the highest mortality in humans compared to other diseases [2] posing an urgent threat to human beings. A common cause of these diseases is the restriction of blood flow to the major arteries in these organs, either by rupture of atherosclerosis plaques, or by capture of emboli from different sources. Such blockade immediately shuts off local blood supply and leads to rapid immune responses or organ disorders.

In vivo models mimicking the blockade of major blood vessels have been used for many decades. Conventionally, these models often require the physical restriction of blood flow of major blood vessels, such as the MCAO (Middle Cerebral Artery Occlusion) model[4] and ligation induced myocardial infarction mode[5]. These models usually cause large areas of tissue ischemia which were associated with significant morbidities on animals. The application of these models has revealed many key responses and mechanisms of cerebral stroke[6; 7; 8; 9] and myocardial infarction[10; 11; 12; 13; 14].

 doi:10.20944/preprints202306.0649.v1

In contrast to major artery blockade, microembolism was more recently proposed. Microembolism is caused by particles with much smaller size (normally <500 um) which are captured in smaller blood vessels[15]. Naturally occurring microemboli can originate from of different sources including platelet fibrin clots, cholesterol[16] or cancerous cells[17] etc.. Although microemboli can arrive in any parts of the body, study of the brain is of most interest. It is known that a large number of microemboli can lead to "warning stroke", which is sometimes referred to as a microstroke or transient ischemic attack (TIA). Its occurrence is regarded as of high risk for future large blockade. Microemboli are more commonly found in patients with cardiovascular diseases, especially arterial atherosclerosis and atrial fibrillation patients. Although microemboli are often found to be asymptotic, it is believed that these patients have a higher risk for silent strokes and cognitive damage[18]. Transcranial Doppler Ultrasound (TCD) has been used to diagnose microemboli in the brain, especially on patients with increased risk for stroke or during cardiovascular interventions[18].

Other than naturally occurring microemboli, new medication strategies exploiting drug-eluting microsphere is under rapid development in recent decades[19; 20]. Microsphere based drugs were already successfully approved to the market[20]. Comparing to the well-studied immune responses caused by major artery blockade, the physiological and immune responses caused by microemboli is less well characterized. In this study, we used fluorescently labeled polystyrene microspheres as the model to mimic microemboli, and sought to address the responses and sequelae of microvascular obstruction. By the use of intravital microscopy, we found interesting monocyte recruitment phenomenon which happens only to the brain but minimally to other organs. Centered on this discovery, this study sought to addressed what monocytes were recruited, and what are the mechanisms behind.

Materials and Methods

Animals

C57BL/6 wild type mice were purchased from Charles Rivers. Transgenic mice CX3CR1$^{gfp/gfp}$ (Cat# 005582) and C3$^{-/-}$ mice (Cat# 003641) were purchased from Jackson lab and breed in SPF level animal facility with controlled temperature (22-24^{o}C), humidity (30-60%) and 12h light/12h dark cycle. For all experiments, we used mice aged 6-12 wk old. Both male and female mice were used. The animal study protocol was approved by the Animal Ethics Committee of Sun Yat-Sen University under protocol number [2018]08–81. Guidelines for the Ethical Review of Laboratory Animal Welfare (GB/ T35892-2018) and institutional ethical guidelines for animal experiments were established by the Fifth Affiliated Hospital of Sun Yat-sen University.

Mouse behavior scoring

Various scoring systems has been developed for evaluating the severity of neurological disorders in rodents. We chose the Bederson scoring to use in this study. The Bederson score grades rodents on a scale of 0-5 from Grade 0 (no defects) to Grade 5 (most severe). Specifically, animals with longitudinal spinning after stroke were scored Grade 4, while those with no movement were scored Grade 5.

Microsphere and treatment

Polystyrene microspheres of 6 μm and 10.00 μm were purchased from Polysciences under trademark Fluoresbrite (6 μm, Cat# 18141; 10.00 μm, Cat# 18142). In this study, we predominantly used intravenously injected polystyrene microspheres as the model to address the host responses. Microspheres were diluted in sterile PBS and injected 5x10^{6} in 200 μl PBS to each mouse. For some experiments, intracarotid injection was performed. Briefly, after anesthesia, the left common carotid artery (CCA) was exposed through a ventral midline incision in the neck. The CCA was then bluntly dissected from surrounding connective tissue. The microspheres were transferred to the cerebral circulation via

Preprints (www.preprints.org) | NOT PEER-REVIEWED | Posted: 8 June 2023 doi:10.20944/preprints202306.0649.v1

the left internal carotid artery by temporary ligating the left external carotid with sutures. A small incision was made in the CCA with fine microsurgical scissors, and a special catheter was connected to a Hamilton syringe and 200 µl of total volume was given at the desired dosage. The catheter was withdrawn and the incision was resealed with cyanoacrylate glue. The surgical wound was sutured, and the mice were closely monitored until recovery after operation.

Fungal strains

In some experiments, *Saccharomyces cerevisiae* was injected instead of microspheres. *S. cerevisiae* S288c were allowed to grow to log phase in yeast growth medium at 30°C with shaking at 200 rpm and harvested by centrifugation at 500 g for 5 min and twice wash with sterile PBS. $5x10^6$ fungal cells in 200 µl PBS was injected to each mouse.

Intravital microscopy

To visualize cell movements in the brain, mice were anesthetized with avertin 300 µl per mice. the transcranial window of around 6 mm was created to allow visualization of the blood vessels on the cortex. The mice were placed on a heating pad to maintain body temperature. The head of the mice was immobilized on a customized imaging stage and placed on the imaging system built upon Nikon Ni microscope equipped with Lumencor SpectraX for fluorescence illumination and PCO EDGE 4.2 camera for detection. Alexa Fluor 647 anti-mouse CD45 antibody (Biolegend Cat#160304) was used to label circulating immune cells. Video tracks were recorded at 1 frame per second. Acquired images were processed with ImageJ software to study the behavior of

Cytokine measurement.

To measure cytokines, the kits were purchased from R&D systems (TNF-α) and eBioscience (IL-1β) following manufactures instructions.

Splenectomy

The splenectomy was performed following established protocol[21]. Briefly, the left side of the abdomen was shaved and disinfected, a 5 mm incision was made to open skin and abdominal cavity. The spleen was carefully exposed and the afferent and efferent vessels were ligated using 4/0 suture before spleen was removed. Abdomen and skin were then surgically closed. Mice were used for experiment two weeks after the surgery.

QPCR

For detection of changes in mRNA transcription, 50 mg tissue were collected for RNA extraction by Trizol (Invitrogen) method. First strand cDNA was synthesized by first strand cDNA synthesis kit (Invitrogen, Catg# 18080051). The primers for qPCR was as below TNF-F: CATCTTCTCAAAATTCGAGTGACAA, TNF-R: TGGGAGTAGACAAGGTACAACCC, and GAPDH-F: CATCACTGCCACCCAGAAGACTG: GAPDH-R: ATGCCAGTGAGCTTCCCGTTCAG.

Immunofluorescence staining

The tissues were removed and frozen in OCT compound (Sakura). Frozen tissue blocks were cut on a cryostat microtome with a thickness set to 7 µm/section; and sections were placed on coated glass slides. Tissue sections were fixed in ice cold acetone for 10 min. After fixation, the samples were blocked by incubation with 5% goat serum for 30 min, followed by incubation with the primary antibody at 4 °C overnight. After three washes with PBS containing 0.05% Tween 20, sections were incubated for 30 min with the fluorescence conjugated second antibodies. After washing, the tissues were stained with DAPI to stain the nuclei and persevered in anti-fade buffer (Invitrogen). The tissue slides were examined under the Zeiss LSM 800 system.

Preprints (www.preprints.org) | NOT PEER-REVIEWED | Posted: 8 June 2023 doi:10.20944/preprints202306.0649.v1

Immune cell isolation and flowcytometry

Mice were euthanized by CO2, the organs were harvested and placed on ice. After collection of all groups, the organs were minced into small pieces <1 mm^3 using fine surgical scissors and digestive with Collagenase IV and DNase I at 37°C for 40 min. The digest was forced through 70 um cell strainer with the help from a 5 ml syringe plunger. The filtrates were centrifuged at 400 g for 5min to remove cell debris. After removal of the supernatant, the cells pellets were resuspended in 2 ml 30% and carefully layered onto 80% Percoll (GE, USA) in 15 ml tube without perturbing the interface, and centrifuged at 1000g for 15 min at room temperature. The cells at the interface between 30% and 80% were collected and washed with flow staining buffer (1% BSA with 0.05% sodium azide). Isolated immune cells enumerated by a hemocytometer and 10^6 cells collected for following steps. Before staining, cells were blocked with Fc receptor blocking antibody at RT for 30 min, and strained with antibodies. All antibodies were purchased from Biolegend. Cells were analyzed by a FACS Aria III machine. 100000 events were recorded and the resulting fcs file was analyzed by Flowjo V10 software.

TNF-α treatment

To study the behavior of monocytes, we isolated spleen monocytes using magnetic isolation kit from Miltenyi (Cat# 130-100-629). Monocytes were treated with or without 10 ng/ml at 37°C for 4 hours and $2x10^6$ cells were infused into mice to evaluate monocyte recruitment.

Antibody treatment

For neutralizing TNF-α in vivo, mice were i.p. injected with 200 μg anti TNF-α antibody (Bioxcell, Cat#: BE0058) 10 min before treatment with microspheres.

Statistics

All data were expressed as mean ± SEM. Statistical significance was performed using Graph-Pad Prism 5 software. For statistics, unpaired two-sided Student's t-test was performed for simple comparison; for comparisons of more than two groups, one-way analysis of variance (ANOVA) was performed followed by Bonferroni's post hoc test to determine significance among groups. In both cases, $p < 0.05$ was considered significant.

Results

Polystyrene microspheres can be mechanically trapped in capillary vessels

To study the results of capillary blockade by microspheres, we injected fluorescence labeled microspheres of 6 μm and 10 μm in diameter into the tail vein of mice and studied their clearance in the circulation and the distribution in different organs. The number of circulating microspheres of both sizes decreased rapidly in the blood steam (Figure 1A). For 6 μm microspheres, only less than 1% remained in the circulating after 10 min. The clearance from circulation is even faster for larger microspheres (Figure 1A). After analysis of organ distribution of microspheres injected through tail vein, it is found that the lung always traps the highest number of microspheres (Figure 1B), This is not surprising since venous blood first pass through the lung. The liver capturing the second largest number of microspheres. Further study demonstrated that microspheres of both sizes injected through the tail vein located in the capillary vessels (Figure 1B). Considering the size of capillary vessels is around 5 μm, we used 6 μm microspheres for the following experiments. The treatment of microspheres at this dosage has minimum effect on the survival (Figure S1A&B) and behavior (Figure S1C) of mice. The arrival of microspheres completely cutoff the movement of red blood cell in that capillary vessel, the movement of blood cells in unaffected vessels were not affected (Figure 1D). Microspheres in the brain, kidney, lung, heart can reside in the capillary for up to 7 days (Figure S1D). Due the existence of the reticuloendothelial system, most microspheres in the liver and spleen

Preprints (www.preprints.org) | NOT PEER-REVIEWED | Posted: 8 June 2023 doi:10.20944/preprints202306.0649.v1

were being engulfed by macrophages, however, in other organs microsphere almost extensively exist by itself (i.e. not being phagocytized) (Figure 1E). Collectively, the introduction of rigid microspheres into the blood stream results in rapid capture of microspheres in capillary beds and blocks local blood cell passing.

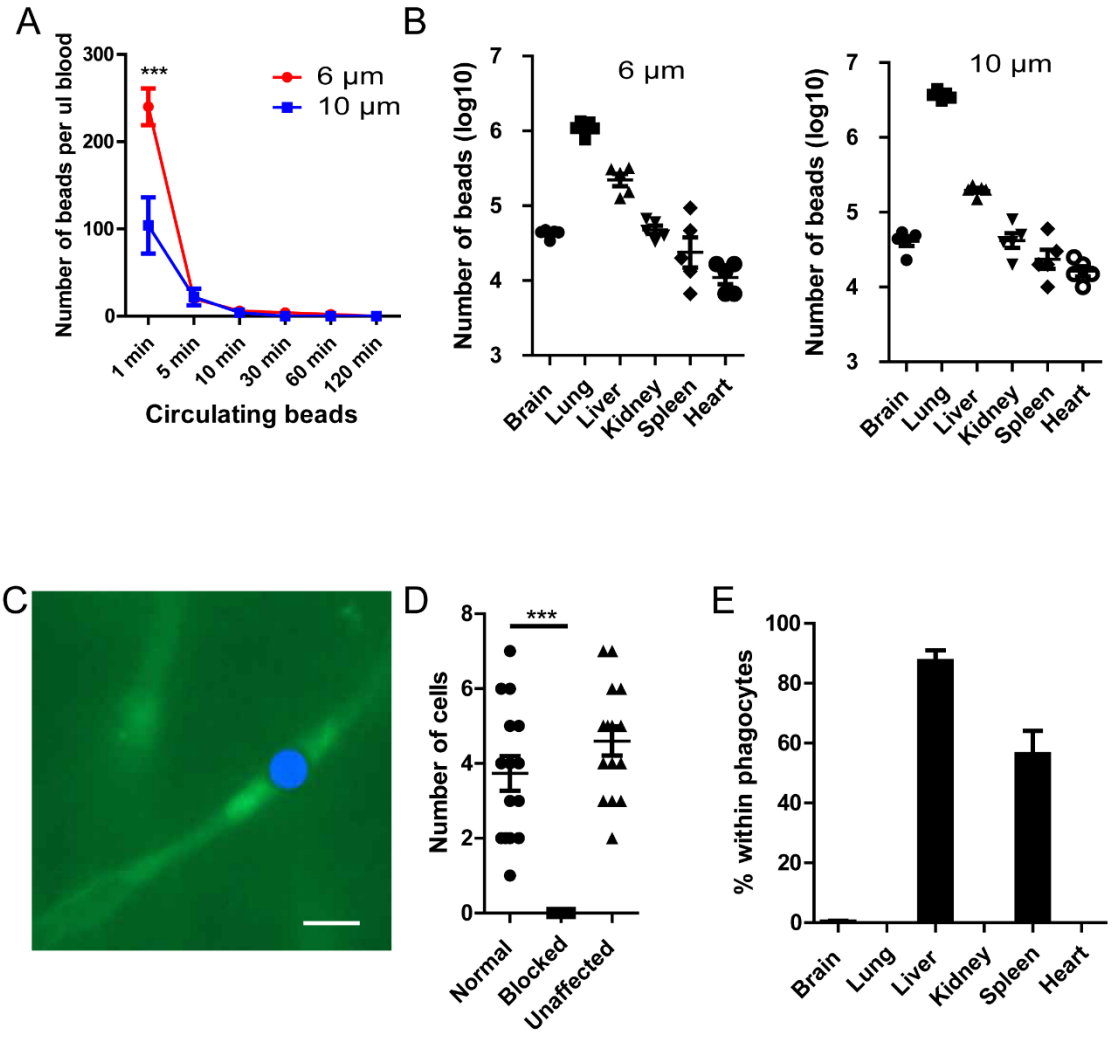

Figure 1. Polystyrene microspheres can be mechanically trapped in capillary vessels.

(A) Microspheres ($5x10^6$) were injected into the tail vein of mice (n=5 in each group), at different time intervals, the microspheres remaining in circulation was evaluated by tail vein blood. (B) The distribution of beads in different organs 2 hours post injection (n=5 in each group). (C) The location of beads in capillary vessels, the FITC-Beads were artificially painted blue for better contrast. Blood vessel is labeled by 70KD FITC-Dextran. (D)The number blood cells passing through a capillary branch per second. (E) The percentage of beads within F4/80+ phagocytes (n=3 in each group). ***, $p<0.001$ by student's *t* test.

Microspheres treatment induced monocyte recruitment in to the brain vasculature

To study the sequela of capillary blockade, we monitored global and local immune responses after microspheres treatment. Serum levels of proinflammatory cytokines including TNF-α and IL-1β are very low (Figure S2) suggesting the polystyrene microspheres are not strongly inflammatory. By immune staining of neutrophils as an indicator of localized inflammation in different organs, we found there is no significant recruitment of neutrophils in most organs at 4 h and 24 h (Figure 2A). The majority of monocytes were seen in the major vessels, with a small percent in the capillary. However, in contrary to

Preprints (www.preprints.org) | NOT PEER-REVIEWED | Posted: 8 June 2023 doi:10.20944/preprints202306.0649.v1

neutrophils, we found a dramatic increase of immune cells recruited to the brain (Figure 2B&2C) demonstrating rolling and crawling behavior. These cells were further demonstrated to be monocytes by the treatment microspheres to reporter mice which has one allele containing CX3CR1 promoter driven GFP expression (Figure 2D). Interestingly, this increase in monocyte is only seen in the brain after microspheres treatment, but not similarly pronounced in other organs (Figure 2E). Analysis of immune cell profile of the brain by flow cytometry confirmed the increase of CX3CR1 positive monocyte (gating strategy shown in Figure S3), and further showed the recruited monocyte has low to intermediate levels of Ly6C expression (Figure 2F&G).

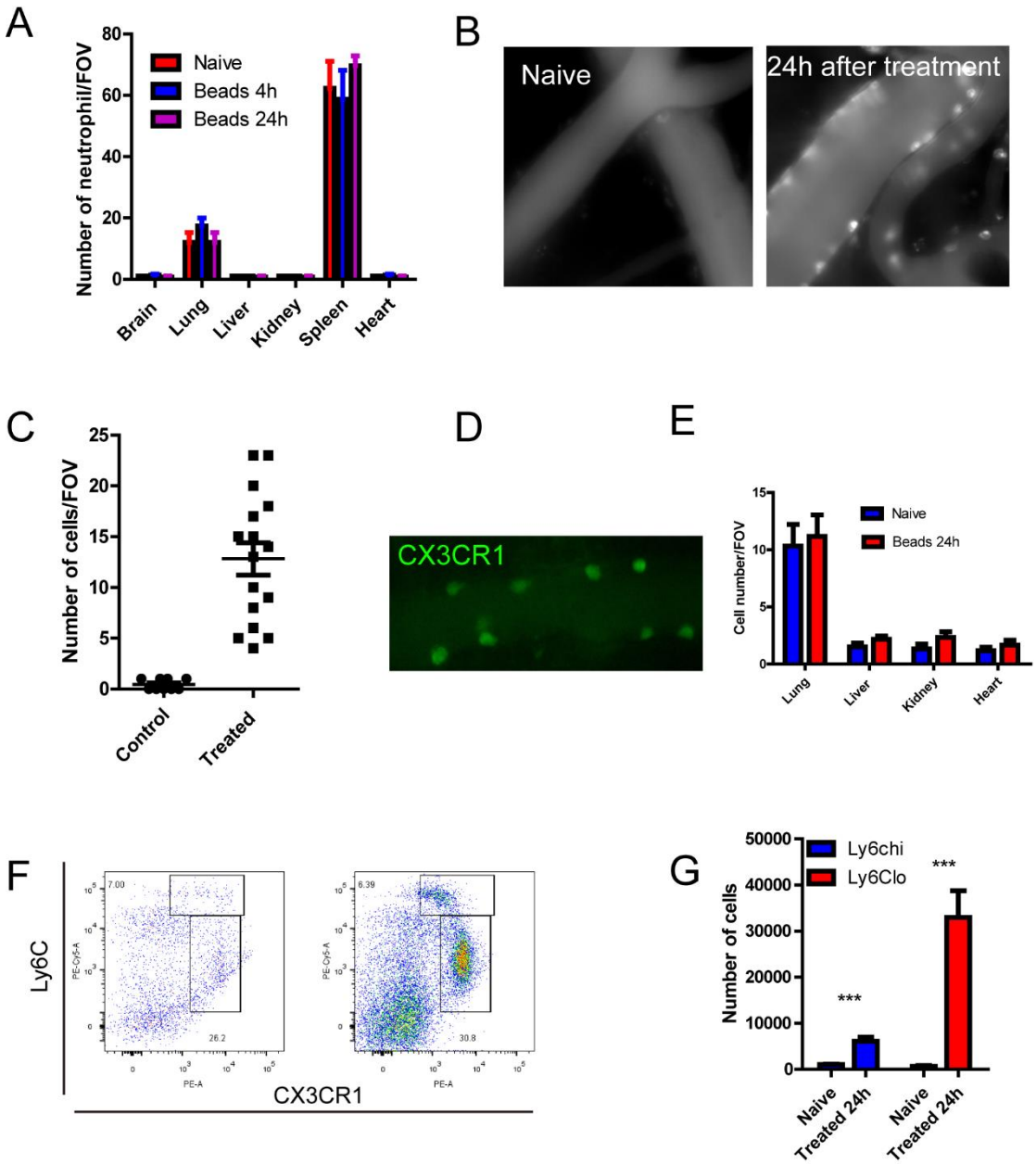

Figure 2. Microspheres treatment induced monocyte recruitment in to the brain vasculature.

(A) Number of neutrophils by immunofluorescence staining tissue sections, size of FOV = 0.2x0.2mm. (B) Recruitment of immune cells in the brain as stained by AF647 labeled CD45. (C) Number of CD45+cells in the circulation, size of FOV is 0.2x0.2 mm. (D) A blood vessel in a CX3CR1$^{gfp/+}$ mice after treatment of microspheres. (E) The number of immune cells in different organs. (F) Flowcytometry analysis of recruited cells in the brain, naive on the left, 24 h after

Preprints (www.preprints.org) | NOT PEER-REVIEWED | Posted: 8 June 2023 doi:10.20944/preprints202306.0649.v1

treatment on the right. (G) Absolute number of monocytes in the brain (n=3 in each group). ***, p<0.001 by student's *t* test.

Spleen is the major source of monocyte recruited to the brain

Under normal situations, the brain harbors very few monocytes of Ly6C^{lo} phenotype. Considering the spleen contains a reservoir of monocytes[22], we questioned whether the monocytes come from the spleen. To confirm the source of monocyte recruited to the brain, we removed the spleen of mice through splenectomy, and treated mice with polystyrene microspheres. It is worth to note that the removal of spleen has little effect on the distribution of microspheres within mouse organs (Figure 3A). We found the removal of spleen dramatically inhibited the recruitment of monocytes to the brain (Figure 3B&C). The imaging results was also confirmed by flowcytometry (Figure 3D). These results suggested that the spleen is the major source of the recruited monocytes in the brain.

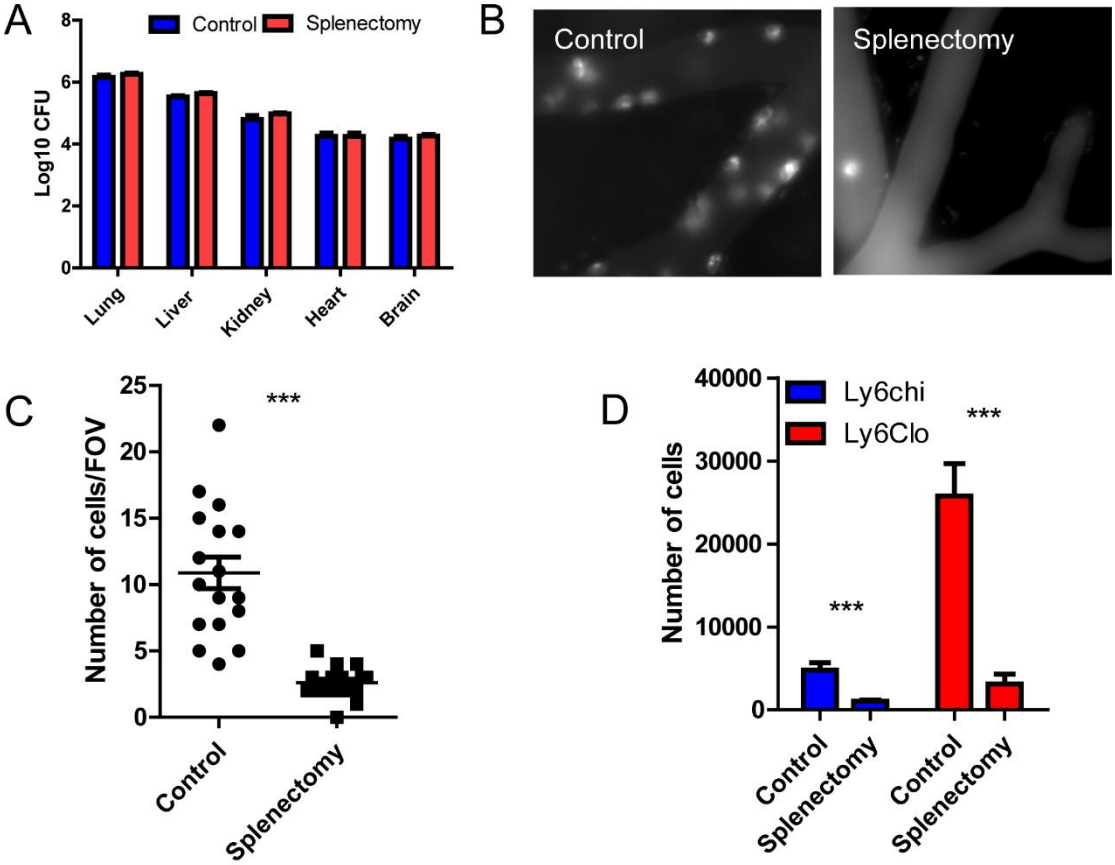

Figure 3. Spleen is the major source of monocyte recruited to the brain.

(A) The distribution of microspheres within different organs comparing control and splenectomized mice. (B) A representative intravital image of the brain vasculature stained by AF647-CD45 in control and splenectomized mice. (C) The number of CD45+ cells in the brain per field of view, size of FOV is 0.2x0.2 mm. (D) Flowcytometry analysis of recruited monocytes in the brain of control and splenectomized mice. ***, p<0.001 by student's *t* test.

CX3CR1 is involved in monocyte recruitment to the brain

CX3CR1 is an important chemokine receptor required for monocyte recruitment in my previous reports. We next questioned whether the loss of this chemokine receptor is involved in monocyte recruitment to the brain. The homologues CX3CR1$^{gfp/gfp}$ mice is considered completely deficient in CX3CR1 expression. Thus, we treated CX3CR1$^{gfp/gfp}$ and CX3CR1$^{gfp/+}$ mice with microspheres and found loss of CX3CR1 resulted in fewer monocytes recruited into the brain (Figure 4A&B). Flowcytometry confirmed the imaging

Preprints (www.preprints.org) | NOT PEER-REVIEWED | Posted: 8 June 2023 doi:10.20944/preprints202306.0649.v1

results (Figure 4C). However, it is worth to mention that CX3CR1 mice has reduced monocyte count in the circulation even under naïve conditions (Figure 4D).

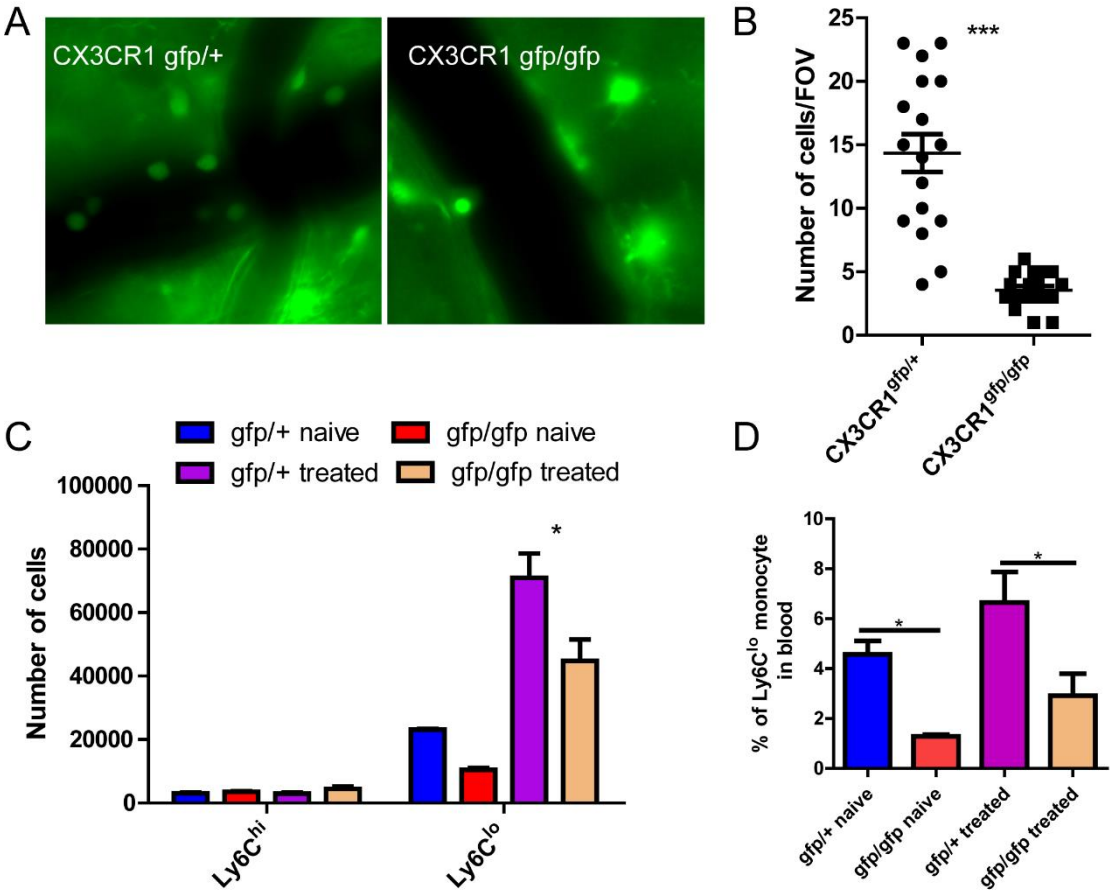

Figure 4. CX3CR1 is involved in monocyte recruitment to the brain.

(A) The representative imaging showing differential recruitment of monocyte in CX3CR1$^{gfp/+}$ and CX3CR1$^{gfp/gfp}$ mice. (B) The number of GFP+ cells in the brain per field of view, size of FOV is 0.2x0.2 mm. (C) Flowcytometry analysis of recruited monocytes in the brain in CX3CR1$^{gfp/+}$ and CX3CR1$^{gfp/gfp}$ mice. (D) The number of circulating monocytes in CX3CR1$^{gfp/+}$ and CX3CR1$^{gfp/gfp}$ mice. *, $p<0.05$ by student's *t* test.

The distinct recruitment of monocyte depends on VCAM-1 expression

It is intriguing that systemically introduced microspheres caused monocyte recruitment in the brain, but not in other organs. We further questioned the mechanisms in the brain that recruited monocytes. Classically, leukocyte recruitment required selectin mediated rolling and integrin mediated adhesion. The interaction of adhesion molecules ICAM-1 and its partner LFA1 mediated the crawling of patrolling monocyte in vascular bed[15]. However, the blood vessels in the brain express neglectable amounts of ICAM-1 both under naïve and microspheres treated conditions (Figure 5A&B), thus discouraging us to believe ICAM-1 is playing a role in monocytes recruitment of the brain. Vascular cell adhesion molecule-1 (VCAM-1) has been shown to mediate monocyte recruitment, so we studied the VCAM-1 expression in different organs by injecting fluorescence labelled antibody, and found VCAM-1 expression is

Preprints (www.preprints.org) | NOT PEER-REVIEWED | Posted: 8 June 2023 doi:10.20944/preprints202306.0649.v1

constitutively expressed on a major portion of brain post-capillary vessels (Figure 5A&B).

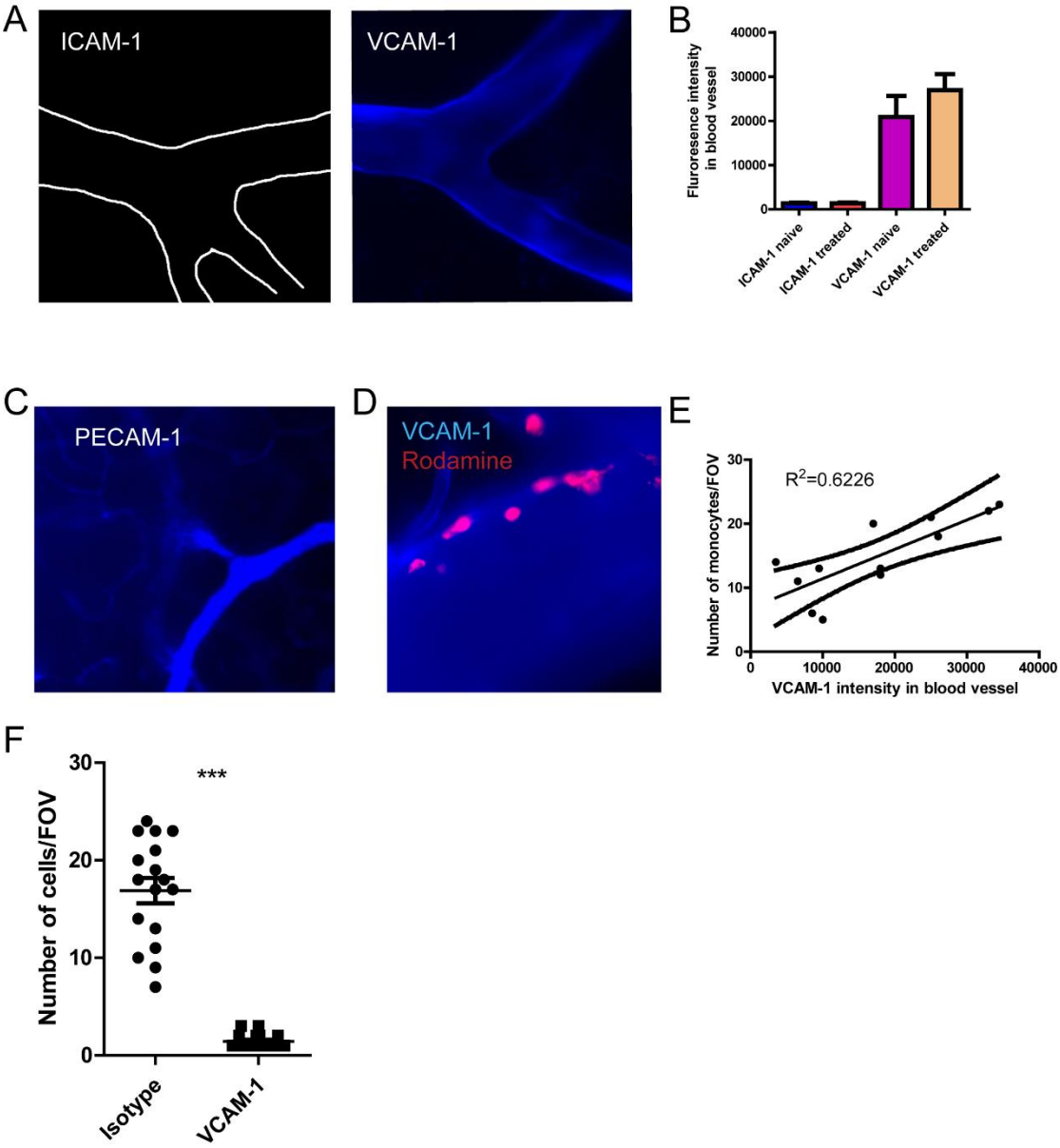

Figure 5. The distinct recruitment of monocyte depends on VCAM-1 expression.

(A) The staining of ICAM-1 and VCAM-1 by injection of AF647 labeled antibodies, and the brain vasculature was visualized using intravital microscopy. (B) The fluorescence intensity of ICAM-1 and VCAM-1 in the different blood vessels of the brain. (C) The staining of PECAM-1by injection of AF647 labeled antibodies showing the capillary vessels. (D) VCAM-1 expression and recruitment of monocyte. （E）The association of VCAM-1 expression and the number of monocytes recruited to that blood vessel. （F) The number of monocytes after the treatment with isotype or VCAM-1 antibody. *, $p<0.05$ by student's *t* test. Scale bar= 20 μm.

Interestingly VCAM-1 is not expressed on capillary vessels, this is in contrast to PECAM-1 which express on both big vessels and capillary vessels (Figure 5C). VCAM-1 express in other organs including the liver, lung, and kidney is low (Figure S4). Monocyte recruitment is strongly associated with the VCAM-1 expression on that particular vessel (Figure 5D&E). We next questioned whether VCAM-1 is involved in the monocyte recruitment in the brain by treatment of mice with VCAM-1 blocking antibody. Treatment of VCAM-1 significantly reduced the number of monocytes recruited in the brain (Figure 5F), while treatment of control antibody has no effect. Collectively, we found a majority of the big blood vessels in the brain constitutively express VCAM-1 and correlate with the recruitment of monocytes.

Preprints (www.preprints.org) | NOT PEER-REVIEWED | Posted: 8 June 2023 doi:10.20944/preprints202306.0649.v1

TNF signaling is crucial for monocyte recruitment to the brain

The well recognized partner of VCAM-1 is integrin VLA-4, which is constitutively expressed on monocytes, but are under "closed" status without stimulation. We inferred that a signal exists that activates monocyte VLA-4. The introduction of exogenous substances often leads to activation of complement system, thus we tested whether there is any complement deposition on microspheres. However, the treatment of complement deficient mice $C3^{-/-}$ mice still retained the monocyte brain recruitment phenomenon (Figure 6A) suggesting complement is not required for monocyte recruitment. It was previously shown that TNF-α signaling can induce activation of integrin, thus we isolated monocyte from the spleen and treated them with recombinant TNF-α in vitro, then infused back into the circulation. We were able to detect increased monocytes in the brain vasculature indicating TNF-α is sufficient to activate monocyte (Figure 6B), As expected. not much monocyte enrichment was observed for mock-treated monocytes. To further establish the role of TNF signaling in vivo, we treated mice with TNF-α neutralizing antibody after microspheres treatment. TNF-α neutralization treatment also largely eliminated the recruitment of monocyte to the brain (Figure 6C).

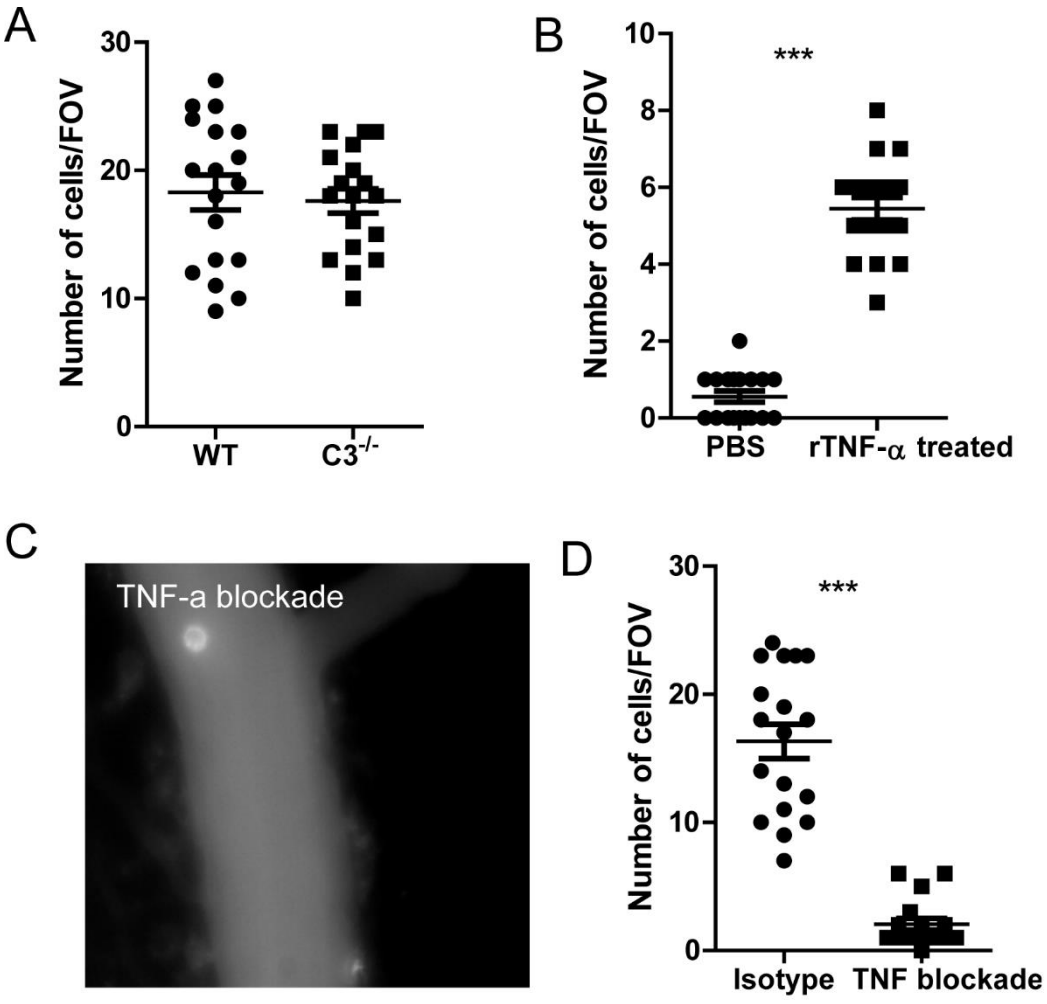

Figure 6. TNF signaling is crucial for monocyte recruitment to the brain.

(A) The recruitment of monocytes into the brain in WT and complement deficient $C3^{-/-}$ mice. (B) Monocytes were isolated from spleen and in vitro stimulated with recombinant mouse TNF-α and then infused back in to the mouse. The brain can immediately see the recruitment of monocytes to the brain. (C) A representative image showing the TNF-α blockade to the recruitment of monocytes. (D) The recruitment of monocytes to the brain after TNF blockade or isotype treatment. mice

Preprints (www.preprints.org) | NOT PEER-REVIEWED | Posted: 8 June 2023 doi:10.20944/preprints202306.0649.v1

were treated with 200 μg anti-TNF-α antibody to neutralize its function. ***, p<0.001 by student's *t* test.

Yeast cells can induce monocyte recruitment

The above results indicated that TNF-α is required for monocyte recruitment, we next questioned whether TNF- α is produced in the brain or in other organs like the spleen? Since ELISA has a low sensitively, qPCR was used to detect the TNF-α mRNAs in the brain and in the spleen, as expected, we detected increased TNF-α expression in the spleen but not in the brain (Figure 7A), suggesting the production and activation of TNF-α may not be from the brain and is more likely in the spleen. To further prove this hypothesis, we injected microspheres to the carotid artery with a dosage comparable to those captured in the brain by i.v. injection. Such injection resulted in the majority of beads being trapped in the brain, but much fewer in other organs. Using intracarotid artery injection, we found monocyte was no long dramatically recruited as before (Figure 7B). This results further indicated that production of TNF-α and activation of monocytes happens somewhere other than the brain, most likely the spleen. Microbes like fungus are of comparable size and have the ability to enter the blood stream and cause diseases. To test whether microbes can induce monocyte recruitment to the brain, we injected mice with Saccharomyces cerevisiae which has an average size of 5-6 μm, and checked monocyte recruitment in the brain, the result showed that such treatment also stimulated monocyte recruitment in the brain. The monocyte recruited to the brain can approach the microspheres that blocks the microcirculation, however, they seemed unable to remove the microemboli (Figure S5).

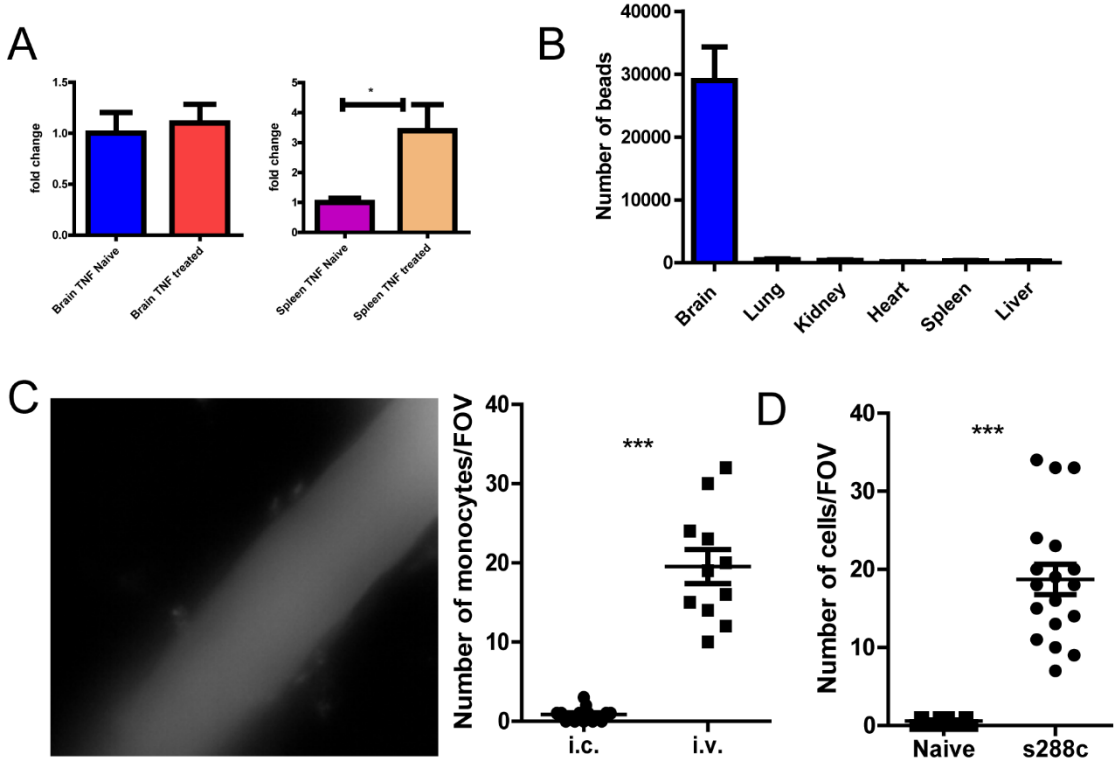

Figure 7. Yeast cells can induce monocyte recruitment.

(A) qPCR detection of TNF-α mRNA in brain and spleen tissues. (B) The distribution of microspheres 2 h after intra carotid injection. (C) The response in mouse brain 24 h after intra carotid injection (left), enumeration on the right. (D) The treatment of mice with fungi *S. cerevisiae* led to recruitment of monocyte into the brain. ***, p<0.001 by student's *t* test.

Discussion

Preprints (www.preprints.org) | NOT PEER-REVIEWED | Posted: 8 June 2023 doi:10.20944/preprints202306.0649.v1

Blood vessels can be clogged by thrombus or embolus in the lumen. Blockade or restriction of normal blood circulation is the culprit of fatal diseases like coronary artery[23] diseases, stroke[1; 9], etc.. These diseases often arise from the result of sudden blockade of major blood vessels. Blockade of major vessels leads to immediate shortage of local blood supply, and often triggers acute consequences including cell death[24; 25], inflammatory cell recruitment[10; 26] which have received extensive study in the past decades. However, the results from blockade of microcirculation are less well characterized. Here we found that microspheres of 6 um injected directly into the circulation can block microcirculation in capillary vessels. This model is in sharp contrast to previous models mimicking the occurrence of major blood vessel blockade by surgical methods[4; 5; 27]. Although microspheres have been used to cause microembolic infarction in animal models, previous studies usually used big-sized microspheres (> 50 μm) which blocks bigger vessels.[28].

In vivo, microemboli predominantly consisted of platelet aggregates, fibrin, cholesterol crystals, tumor cells [15; 29]. Microemboli can happen in the brain which results in disrupt the blood-brain barrier and impairs cognition [15; 18; 30], and also in the heart[29], the lung[31] etc. Mechanical stress from hemodynamic perturbations or interventional manipulation of epicardial coronary atherosclerotic plaques with inflammatory destabilization can release particulate debris and other thrombotic materials into circulation[29]. A pathological study of COVID-19 patients revealed that microthrombi as a major cause of cardiac injury [31]. Blocking microcirculation using our experimental dosage did not induce apparent morbidity in mice, however, it has to be admitted that we did not perform in depth and long-term study on neurological damage. Blocking microcirculation may still have profound neurological disorders in the long run. Previously, it was found that short of blood supply can lead to rapid loss of spine and dendrite structure which can be reversible[32]. In fact, the occlusion of microvessels is able to cause sufficient hypoxia which results in transient focal dendritic spine loss[16]. Thus, focal change in neuron is also likely to happen in our model.

Previously, Carson et al. reported an interesting and important phenomenon which showed microemboli trapped in the microvessels can be expelled out of the vessel into brain perivascular parenchyma resulting in recanalization of the circulation after 48 hours[16]. They further showed the extravasation is dependent on metalloprotease activities[16]. Treatment with MMP-2/9 inhibitor SB-3CT suppressed extravasation of the microemboli. The study used microemboli with different compositions including fibrin, cholesterol and microsphere and found the expel of microemboli happens regardless of the microemboli composition. The authors infer that pericyte may be involved in providing the force of extravasation[16; 33]. It should be noted that the size they used is slightly bigger than those used in our study (10-15 μm, comparing to 6 μm). This size difference can make a big difference in following responses, because microspheres of 6 μm can allow blockade of the smallest level of capillary vessels while microspheres bigger than 10 μm may not reach that level. Our data showed that small microspheres are not expelled as efficiently as those reported. Whether different levels of capillary have different expel efficiency need further study.

The study of microsphere triggered response has further meaning. Nowadays more and more microsphere bases drugs are being developed. Among all the approaches microspheres are more convenient as the drug is slowly released from the polymeric matrix and the polymers used are mostly biodegradable and possess no side effects. Therefore, microspheres can be used in various medicinal departments such as oncology, gynecology, radiology, pulmonary, cardiology, diabetes, and vaccine therapy. Drug-eluting embolic (DEE) microspheres, or drug-eluting microspheres (DEB) which were delivered by transarterial chemoembolization (TACE) are used as a drug delivery vehicle to stop blood flow to tumors [20]. Microspheres to enhance drug delivery to the liver dates back several decades[34]. As carriers of drug, the distribution of microspheres significantly affects the location of the drug. The sizes of microsphere have a huge effect on the distribution of microspheres. Transcatheter arterial chemoembolization (TACE) is a minimally invasive

 doi:10.20944/preprints202306.0649.v1

procedure performed in interventional radiology to restrict a tumor 's blood supply. Small embolic particles coated with chemotherapeutic drugs are injected selectively through a catheter into an artery directly supplying the tumor. Artificial drug-eluting embolic microspheres has been utilized as therapeutic strategies to stop blood flow to tumors via transarterial chemoembolization[20]. TACE has become one of the preferred choices for advanced liver cancer patients PVA, gelatin, and alginate microspheres[19]. Drug-eluting embolic microspheres has already been commercialized for cancer therapy, which incorporates doxorubicin etc..[20]. Chemoembolization therapy has been used for hepatocellular carcinoma treatment with drug eluting microspheres[35]. Thus, characterization of the resulting responses in the local environment is important for understanding the sized effects of microsphere-based drugs.

TNF-α and VCAM-1 have been indicated to be involved in cell recruitment and disease progression. For example, TNF-α treatment of EPCs can lead to increased adhesion by increasing bond affinity[36] and lipid-induced endothelial VCAM-1 was shown to promote nonalcoholic steatohepatitis pathogenesis[37]. Although, inflammatory signals can trigger the expression of VCAM-1 on endothelial cells[38], in our model, we failed to detect systematically increased TNF-α in serum by ELISA, thus indicating the lack of systematic inflammation. VCAM-1 expression can also be regulated by shear force[39]. However, we found that the VCAM-1 molecules are constitutively expressed on brain capillary vessels. Consistent with our report, previous studies showed that selective targeting of VCAM-1 liposome to inflamed cerebral vasculature dramatically enhanced the blood-brain barrier targeting than ICAM-1[40].The expression of VCAM-1 explains the differential recruitment of monocytes in different organs.

The spleen is a large reservoir of monocytes that outnumbers blood monocytes which can be recruited during inflammation. Splenic monocytes cluster in the subcapsular red pulp[22]. Previous studies mostly focused on the recruitment of Ly6C^{hi} monocytes. One day after coronary ligation, we observed reduced numbers of monocytes in the subcapsular red pulp of the spleen. Monocytes in the spleen are very similar in phenotype to blood-derived monocytes and are mobilized to the injured heart, where they represent a large fraction of total monocytes that are recruited [22]. The microspheres induced monocyte recruitment is in striking contrast to the LPS [41] induced inflammation of the brain, in the later models neutrophils arrived in a much faster fashion (within 4 hours). A previous work identified the recruitment of Ly6C^{lo} monocytes in Alzheimer mice model that played an important role in clearance of the amyloid-β load in the brain cortex and hippocampus[42]. Amyloid-β can be recognized by many pattern recognition receptors which may further activate TNF-α signaling [43]. Thus, our work provided new potential mechanisms for the monocyte recruitment in this disease model.

In conclusion, we found polystyrene microspheres of 6um size can completely block the blood flow of the capillary, and result in recruitment of monocyte with intermediate levels of Ly6C to the brain. VCAM-1 is the molecule that dictates the differential recruitment of monocytes. The activation of monocytes requires the TNF-α signaling by stimulating the monocyte by polystyrene microspheres. The study model in this although seemingly artificially, helps to address the sequela of capillary blockade in different organs. Such situation can be naturally occurring during diseased conditions or happen during future medication. This study emphasized the importance of organ specific monocyte responses to stimuli which has importance the understanding of monocyte role in major diseases.

Supplementary Materials: The following supporting information can be downloaded at the website of this paper posted on Preprints.org , Figure S1: Mouse behavior after microsphere treatment.; Figure S2: The detection of TNF-α and IL-1β production using ELISA. 10 μg/ml final concentration of LPS was used as control.; Figure S3: The gating strategy for neutrophil P1, Ly6C^{hi} monocyte P2 and Ly6C^{lo} monocyte P3.; Figure S4: The VCAM-1 intensity on different organs studied by fluorescence microscope. Figure S5: Monocytes were frequently seen approaching the microsphere.

Author Contributions: Conceptualization, Wei-Wei Zhu and Lin Zhao; Data curation, Junyao Wang and Qiming Dong; Formal analysis, Wei-Wei Zhu and Jian Chen; Funding acquisition, Jian Chen; Methodology, Lin Zhao and Jian Chen; Project administration, Lin Zhao; Resources, Junyao Wang; Supervision, Lin Zhao and Jian Chen; Writing – original draft, Wei-Wei Zhu; Writing – review & editing, Junyao Wang and Qiming Dong.

Funding: This study was supported by the National Natural Science Foundation of China Youth Program (No. 82100484).

Conflicts of Interest: The authors declare no conflict of interest.

References

[1] B.C.V. Campbell, D.A. De Silva, M.R. Macleod, S.B. Coutts, L.H. Schwamm, S.M. Davis, and G.A. Donnan, Ischaemic stroke. Nat Rev Dis Primers 5 (2019) 70.
[2] G.B.D. Mortality, and C. Causes of Death, Global, regional, and national age-sex specific all-cause and cause-specific mortality for 240 causes of death, 1990-2013: a systematic analysis for the Global Burden of Disease Study 2013. Lancet 385 (2015) 117-71.
[3] M.V. Huisman, S. Barco, S.C. Cannegieter, G. Le Gal, S.V. Konstantinides, P.H. Reitsma, M. Rodger, A. Vonk Noordegraaf, and F.A. Klok, Pulmonary embolism. Nat Rev Dis Primers 4 (2018) 18028.
[4] C.J. Sommer, Ischemic stroke: experimental models and reality. Acta Neuropathologica 133 (2017) 245-261.
[5] M.L. Lindsey, K.R. Brunt, J.A. Kirk, P. Kleinbongard, J.W. Calvert, L.E.D. Bras, K.Y. DeLeon-Pennell, D.P. Del Re, N.G. Frangogiannis, S. Frantz, R.J. Gumina, G.V. Halade, S.P. Jones, R.H. Ritchie, F.G. Spinale, E.B. Thorp, C.M. Ripplinger, and Z. Kassiri, Guidelines for in vivo mouse models of myocardial infarction. Am J Physiol-Heart C 321 (2021) H1056-H1073.
[6] X. Urra, A. Cervera, V. Obach, N. Climent, A.M. Planas, and A. Chamorro, Monocytes are major players in the prognosis and risk of infection after acute stroke. Stroke 40 (2009) 1262-8.
[7] A. ElAli, and N. Jean LeBlanc, The Role of Monocytes in Ischemic Stroke Pathobiology: New Avenues to Explore. Front Aging Neurosci 8 (2016) 29.
[8] W. Zhang, J. Zhao, R. Wang, M. Jiang, Q. Ye, A.D. Smith, J. Chen, and Y. Shi, Macrophages reprogram after ischemic stroke and promote efferocytosis and inflammation resolution in the mouse brain. CNS Neurosci Ther 25 (2019) 1329-1342.
[9] D. Han, H. Liu, and Y. Gao, The role of peripheral monocytes and macrophages in ischemic stroke. Neurol Sci 41 (2020) 3589-3607.
[10] K.I. Mentkowski, L.M. Euscher, A. Patel, B.R. Alevriadou, and J.K. Lang, Monocyte recruitment and fate specification after myocardial infarction. Am J Physiol Cell Physiol 319 (2020) C797-C806.
[11] C. Peet, A. Ivetic, D.I. Bromage, and A.M. Shah, Cardiac monocytes and macrophages after myocardial infarction. Cardiovasc Res 116 (2020) 1101-1112.
[12] T. Heidt, G. Courties, P. Dutta, H.B. Sager, M. Sebas, Y. Iwamoto, Y. Sun, N. Da Silva, P. Panizzi, A.M. van der Laan, F.K. Swirski, R. Weissleder, and M. Nahrendorf, Differential contribution of monocytes to heart macrophages in steady-state and after myocardial infarction. Circ Res 115 (2014) 284-95.
[13] F. Leuschner, P.J. Rauch, T. Ueno, R. Gorbatov, B. Marinelli, W.W. Lee, P. Dutta, Y. Wei, C. Robbins, Y. Iwamoto, B. Sena, A. Chudnovskiy, P. Panizzi, E. Keliher, J.M. Higgins, P. Libby, M.A. Moskowitz, M.J. Pittet, F.K. Swirski, R. Weissleder, and M. Nahrendorf, Rapid monocyte kinetics in acute myocardial infarction are sustained by extramedullary monocytopoiesis. J Exp Med 209 (2012) 123-37.
[14] H. Tsujioka, T. Imanishi, H. Ikejima, A. Kuroi, S. Takarada, T. Tanimoto, H. Kitabata, K. Okochi, Y. Arita, K. Ishibashi, K. Komukai, H. Kataiwa, N. Nakamura, K. Hirata, A. Tanaka, and T. Akasaka, Impact of heterogeneity of human peripheral blood monocyte subsets on myocardial salvage in patients with primary acute myocardial infarction. J Am Coll Cardiol 54 (2009) 130-8.
[15] J.H. Rapp, X.M. Pan, M. Neumann, M. Hong, K. Hollenbeck, and J. Liu, Microemboli composed of cholesterol crystals disrupt the blood-brain barrier and reduce cognition. Stroke 39 (2008) 2354-2361.
[16] C.K. Lam, T. Yoo, B. Hiner, Z.Q. Liu, and J. Grutzendler, Embolus extravasation is an alternative mechanism for cerebral microvascular recanalization. Nature 465 (2010) 478-U101.
[17] A. Carlsson, V.S. Nair, M.S. Luttgen, K.V. Keu, G. Horng, M. Vasanawala, A. Kolatkar, M. Jamali, A.H. Iagaru, W. Kuschner, B.W. Loo, Jr., J.B. Shrager, K. Bethel, C.K. Hoh, L. Bazhenova, J. Nieva, P. Kuhn, and S.S. Gambhir, Circulating tumor microemboli diagnostics for patients with non-small-cell lung cancer. J Thorac Oncol 9 (2014) 1111-9.
[18] D. Russell, Cerebral microemboli and cognitive impairment. J Neurol Sci 203-204 (2002) 211-4.
[19] D.W. Wang, Q.R. Wu, R. Guo, C.N. Lu, M. Niu, and W. Rao, Magnetic liquid metal loaded nano-in-micro spheres as fully flexible theranostic agents for SMART embolization. Nanoscale 13 (2021) 8817-8836.
[20] A.S. Mikhail, A.H. Negussie, M. Mauda-Havakuk, J.W. Owen, W.F. Pritchard, A.L. Lewis, and B.J. Wood, Drug-eluting embolic microspheres: State-of-the-art and emerging clinical applications. Expert Opin Drug Deliv 18 (2021) 383-398.
[21] S.W.C. Li, A.D. Rangel, and M.H. Kabeer, Precision Technique for Splenectomy Limits Mouse Stress Responses for Accurate and Realistic Measurements for Investigating Inflammation and Immunity. Bio-Protocol 9 (2019).
[22] F.K. Swirski, M. Nahrendorf, M. Etzrodt, M. Wildgruber, V. Cortez-Retamozo, P. Panizzi, J.L. Figueiredo, R.H. Kohler, A. Chudnovskiy, P. Waterman, E. Aikawa, T.R. Mempel, P. Libby, R. Weissleder, and M.J. Pittet, Identification of Splenic Reservoir Monocytes and Their Deployment to Inflammatory Sites. Science 325 (2009) 612-616.
[23] P. Libby, and P. Theroux, Pathophysiology of coronary artery disease. Circulation 111 (2005) 3481-8.

 doi:10.20944/preprints202306.0649.v1

[24] A. Sendoel, and M.O. Hengartner, Apoptotic Cell Death Under Hypoxia. Physiology 29 (2014) 168-176.
[25] C.R. Lenihan, and C.T. Taylor, The impact of hypoxia on cell death pathways. Biochem Soc T 41 (2013) 657-663.
[26] J. Lehmann, W. Hartig, A. Seidel, C. Fuldner, C. Hobohm, J. Grosche, M. Krueger, and D. Michalski, Inflammatory cell recruitment after experimental thromboembolic stroke in rats. Neuroscience 279 (2014) 139-54.
[27] J.M. Jia, P.D. Chowdary, X. Gao, B. Ci, W. Li, A. Mulgaonkar, E.J. Plautz, G. Hassan, A. Kumar, A.M. Stowe, S.H. Yang, W. Zhou, X. Sun, B. Cui, and W.P. Ge, Control of cerebral ischemia with magnetic nanoparticles. Nat Methods 14 (2017) 160-166.
[28] O. Mayzel-Oreg, T. Omae, M. Kazemi, F. Li, M. Fisher, Y. Cohen, and C.H. Sotak, Microsphere-induced embolic stroke: an MRI study. Magn Reson Med 51 (2004) 1232-8.
[29] P. Kleinbongard, and G. Heusch, A fresh look at coronary microembolization. Nature Reviews Cardiology 19 (2022) 265-280.
[30] M. Siebler, A. Kleinschmidt, M. Sitzer, H. Steinmetz, and H.J. Freund, Cerebral microembolism in symptomatic and asymptomatic high-grade internal carotid artery stenosis. Neurology 44 (1994) 615-8.
[31] D. Pellegrini, R. Kawakami, G. Guagliumi, A. Sakamoto, K. Kawai, A. Gianatti, A. Nasr, R. Kutys, L. Guo, A. Cornelissen, L. Faggi, M. Mori, Y. Sato, I. Pescetelli, M. Brivio, M. Romero, R. Virmani, and A.V. Finn, Microthrombi as a Major Cause of Cardiac Injury in COVID-19 A Pathologic Study. Circulation 143 (2021) 1031-1042.
[32] S. Zhang, J. Boyd, K. Delaney, and T.H. Murphy, Rapid reversible changes in dendritic spine structure in vivo gated by the degree of ischemia. J Neurosci 25 (2005) 5333-8.
[33] C.M. Peppiatt, C. Howarth, P. Mobbs, and D. Attwell, Bidirectional control of CNS capillary diameter by pericytes. Nature 443 (2006) 700-4.
[34] K.F. Aronsen, C. Hellekant, J. Holmberg, U. Rothman, and H. Teder, Controlled blocking of hepatic artery flow with enzymatically degradable microspheres combined with oncolytic drugs. Eur Surg Res 11 (1979) 99-106.
[35] M. Varela, M.I. Real, M. Burrel, A. Forner, M. Sala, M. Brunet, C. Ayuso, L. Castells, X. Montana, J.M. Llovet, and J. Bruix, Chemoembolization of hepatocellular carcinoma with drug eluting beads: efficacy and doxorubicin pharmacokinetics. J Hepatol 46 (2007) 474-81.
[36] A.R. Prisco, M.R. Prisco, B.E. Carlson, and A.S. Greene, TNF-alpha increases endothelial progenitor cell adhesion to the endothelium by increasing bond expression and affinity. Am J Physiol Heart Circ Physiol 308 (2015) H1368-81.
[37] K. Furuta, Q. Guo, K.D. Pavelko, J.H. Lee, K.D. Robertson, Y. Nakao, J. Melek, V.H. Shah, P. Hirsova, and S.H. Ibrahim, Lipid-induced endothelial vascular cell adhesion molecule 1 promotes nonalcoholic steatohepatitis pathogenesis. J Clin Invest 131 (2021).
[38] R.M. Carr, VCAM-1: closing the gap between lipotoxicity and endothelial dysfunction in nonalcoholic steatohepatitis. Journal of Clinical Investigation 131 (2021).
[39] P.L. Walpola, A.I. Gotlieb, M.I. Cybulsky, and B.L. Langille, Expression of ICAM-1 and VCAM-1 and monocyte adherence in arteries exposed to altered shear stress. Arterioscler Thromb Vasc Biol 15 (1995) 2-10.
[40] O.A. Marcos-Contreras, C.F. Greineder, R.Y. Kiseleva, H. Parhiz, L.R. Walsh, V. Zuluaga-Ramirez, J.W. Myerson, E.D. Hood, C.H. Villa, I. Tombacz, N. Pardi, A. Seliga, B.L. Mui, Y.K. Tam, P.M. Glassman, V.V. Shuvaev, J. Nong, J.S. Brenner, M. Khoshnejad, T. Madden, D. Weissmann, Y. Persidsky, and V.R. Muzykantov, Selective targeting of nanomedicine to inflamed cerebral vasculature to enhance the blood-brain barrier. Proc Natl Acad Sci U S A 117 (2020) 3405-3414.
[41] H. Zhou, B.M. Lapointe, S.R. Clark, L. Zbytnuik, and P. Kubes, A requirement for microglial TLR4 in leukocyte recruitment into brain in response to lipopolysaccharide. Journal of Immunology 177 (2006) 8103-8110.
[42] J.P. Michaud, M.A. Bellavance, P. Prefontaine, and S. Rivest, Real-Time In Vivo Imaging Reveals the Ability of Monocytes to Clear Vascular Amyloid Beta. Cell Reports 5 (2013) 646-653.
[43] F. Leng, and P. Edison, Neuroinflammation and microglial activation in Alzheimer disease: where do we go from here? Nat Rev Neurol 17 (2021) 157-172.